

**Neutrino scattering rates in neutron star matter with  $\Delta$  isobars**YanJun Chen,<sup>1,\*</sup> Hua Guo,<sup>1,3,4</sup> and Yuxin Liu<sup>2,3,4,†</sup><sup>1</sup>*Department of Technical Physics, Peking University, Beijing 100871, China*<sup>2</sup>*Department of Physics, Peking University, Beijing 100871, China*<sup>3</sup>*The MOE Key Laboratory of Heavy Ion Physics, Peking University, Beijing 100871, China*<sup>4</sup>*Center of Theoretical Nuclear Physics, National Laboratory of Heavy Ion Accelerator, Lanzhou 730000, China*

(Received 16 July 2006; revised manuscript received 7 December 2006; published 22 March 2007)

We take the  $\Delta$ -isobar degrees of freedom into account in neutron star matter and evaluate their contributions to neutrino scattering cross sections and mean free paths. The neutron star matter is described by means of an effective hadronic model in the relativistic mean-field approximation. It is found that  $\Delta$  isobars may be present in neutron stars. The electron chemical potential does not decrease and the neutrino abundance does not increase with the increase of the density when neutrinos are trapped in the matter with  $\Delta$  isobars. The large vector coupling constant between the  $\Delta^-$  and neutrino and the high spin of the  $\Delta$  influence significantly the neutrino scattering cross section and lead the contribution of the  $\Delta^-$  to the dominance of the scattering rates. In neutrino-trapped case, the presence of  $\Delta$ s causes the neutrino mean free path to decrease drastically compared to that in the matter in which baryons are only nucleons.

DOI: [10.1103/PhysRevC.75.035806](https://doi.org/10.1103/PhysRevC.75.035806)

PACS number(s): 26.60.+c, 97.60.Jd, 21.65.+f, 13.15.+g

**I. INTRODUCTION**

Theoretical investigations have shown rich structures in hadronic matter at high densities or high temperatures that are expected to be found in experiments of relativistic heavy-ion collisions or some astronomical observables, such as neutron stars. Some articles [1,2] have shown that there may exist stable  $\Delta$ -excited nuclear matter at high densities  $\rho \approx (3 \sim 5)\rho_0$  ( $\rho_0$  is the saturation density of nuclear matter) in the framework of the nonlinear Walecka models and the influences of the  $\Delta$ -excited nuclear matter on the properties of neutron stars have been discussed roughly in Ref. [3] within a chiral effective Lagrangian.

It has been well established that neutron star matter is not pure neutron matter, but probably with quite complicated components, including hyperons, condensates of  $K^-$ , and/or  $\pi^-$ , even quarks and so on (see, for example, Refs. [4–7] and references therein). For  $\Delta$  isobars, Glendenning and collaborators [8,9] once made a specific choice of the couplings, i.e., the  $\Delta$ -isobar-meson couplings are taken to be equal to that between nucleon and the mesons, and showed that the  $\Delta$  isobars emerge at a too-high baryon density to affect neutron stars. However, Jin's work in the framework of finite-density quantum chromodynamics (QCD) sum rules [10] predicts that the coupling between the  $\Delta$  isobar and the scalar meson is stronger and that between the  $\Delta$  isobar and vector mesons is weaker than those between nucleon and the corresponding mesons, respectively. Furthermore, a triangle relation for the  $\Delta$ -isobar coupling constants has been proposed by Kosov and collaborators [11] and shown that the  $\Delta$ -isobar coupling constants can change in a proper range. It means then whether stable  $\Delta$ -excited nuclear matter exists and whether the  $\Delta$  isobars affect the property of neutron stars or not are still a

controversial issue because little is known about the coupling constants of the  $\Delta$  with the scalar and vector mesons. In any case, there have been some discussions on the existence of the  $\Delta$  isobars and the effects on the properties of neutron stars (see, for example, Refs. [3,12,13]). It looks that it is imperative to study the related problems with more profound coupling constants given in fundamental investigations.

Conversely, it has been well known that ordinary matter is transparent to neutrinos; however, the transport properties of neutrinos may play an essential role in the core-collapse supernova explosion and the formation of neutron stars. The important theoretical input of the neutrino transportation is the opacity to neutrinos. There have been lots of works to study the neutrino opacity in dense matter involving both the charged-current absorption and neutral-current scattering reactions on baryons and leptons (see, for instance, Refs. [14–17] and references therein). The neutrino opacity could be modified by interactions of the ambient matter. Sawyer [18,19] and Iwamoto and collaborator [20] have explored the mean free path of neutrinos in dense matter with the nonrelativistic descriptions of nuclear medium and the neutrino scattering cross section has been evaluated with the relativistic framework based on effective Lagrangian models in the mean-field approximation [21–23]. Reddy *et al.* [15–17] have carried out some nonrelativistic and relativistic calculations in protoneutron stars. The components of neutron stars may also affect the opacity. And it has been shown that the presence of hyperons influences the evolution of protoneutron stars [16,24]. The  $\Delta$  isobars, as new possible components of neutron star matter, may affect the neutrino opacity and in turn should be investigated as well.

In the present work, we study the existence of  $\Delta$  isobars in neutron star matter and its effects on the neutrino scattering rates and the neutrino opacity in an effective hadronic model with the coupling constants between the  $\Delta$ s and the mesons being taken as those given in finite-density QCD sum rules. It is organized as follows. In Sec. II, we describe briefly

\*Electronic address: chenyj@pku.edu.cn

†Electronic address: yxliu@pku.edu.cn

the formalism for evaluating the composition of neutron star matter and the neutral-current reactions of neutrinos. In Sec. III, we represent our calculated results and give some discussions. Finally, we summarize our work and give some remarks in Sec. IV.

## II. THE FORMALISM

It has been known that the relativistic mean-field approximation (RMFA) is quite successful in describing the property of normal nuclear matter (see, for example, Ref. [25]). We then describe the neutron star matter with  $\Delta$  isobars by implementing the RMFA in which baryons interact with each other via the exchange of  $\sigma$ ,  $\omega$ , and  $\rho$  mesons. The full Lagrangian density can then be written as

$$L = L_N + L_\Delta + L_l. \quad (1)$$

To highlight the effects of the  $\Delta$ s, we incorporate here only the  $\Delta$ s and nucleons but do not include the hyperon degrees of freedom in Eq. (1). Then the  $L_N$  contains only nucleon and meson sectors and reads [25]

$$\begin{aligned} L_N = & \bar{N}(i\gamma_\mu \partial^\mu - M_N + g_{\sigma N}\sigma - g_{\omega N}\gamma_\mu \omega^\mu \\ & - g_{\rho N}\gamma_\mu \vec{\tau} \cdot \vec{\rho}^\mu)N - \frac{1}{4}w_{\mu\nu}w^{\mu\nu} + \frac{1}{2}m_\omega^2\omega_\mu\omega^\mu \\ & - \frac{1}{4}\vec{\rho}_{\mu\nu}\vec{\rho}^{\mu\nu} + \frac{1}{2}m_\rho^2\vec{\rho}_\mu\vec{\rho}^\mu + \frac{1}{2}\partial_\mu\sigma\partial^\mu\sigma + \frac{1}{2}m_\sigma^2\sigma^2 \\ & - \frac{1}{3}bM_N(g_{\sigma N}\sigma)^3 - \frac{1}{4}c(g_{\sigma N}\sigma)^4, \end{aligned} \quad (2)$$

where  $N(N = p, n)$  denotes the Dirac spinor of nucleon.  $\vec{\tau}$  is the isospin operator of the nucleon. The field tensors for the  $\omega$  and  $\rho$  mesons are  $w_{\mu\nu} \equiv \partial_\mu\omega_\nu - \partial_\nu\omega_\mu$ ,  $\vec{\rho}_{\mu\nu} \equiv \partial_\mu\vec{\rho}_\nu - \partial_\nu\vec{\rho}_\mu$ , respectively.

As for the  $\Delta$  isobars, we take them as separate degrees of freedom. It is well known that thus far there is no relativistic quantum theory for the  $\Delta$  as a spin 3/2 field without any inconsistency when imposing other fields such as the ones with electromagnetic interaction [26]. Moreover, following the Rarita-Schwinger formalism [27], the spin 3/2 particle, described by means of a vector spinor state, has off-shell spin 1/2 sector. To avoid these complicated problems, we take only the on-shell  $\Delta$ s into account and the mass of the  $\Delta$ s can be substituted by the effective one in the RMFA. The Lagrangian density concerning the  $\Delta$  isobars can then be expressed as

$$L_\Delta = \bar{\Delta}_\mu[i\gamma^{\mu\nu\alpha}D_\alpha - (M_\Delta - g_{\sigma\Delta}\sigma)\gamma^{\mu\nu}]\Delta_\nu, \quad (3)$$

where  $\Delta_\mu(\Delta = \Delta^{++}, \Delta^\pm, \text{ and } \Delta^0)$  is the Rarita-Schwinger spinor for the  $\Delta$  [27].  $D_\alpha = \partial_\alpha + ig_{\omega\Delta}\omega^\mu + ig_{\rho\Delta}\vec{T} \cdot \vec{\rho}^\mu$  with  $\vec{T}$  being the isospin operator of the  $\Delta$ . Here, two totally antisymmetric products of  $\gamma$  matrices are involved, which read explicitly

$$\begin{aligned} \gamma^{\mu\nu} &= \frac{1}{2}[\gamma^\mu, \gamma^\nu], \\ \gamma^{\mu\nu\alpha} &= \frac{1}{2}\{\gamma^{\mu\nu}, \gamma^\alpha\} = i\epsilon^{\mu\nu\alpha\beta}\gamma_\beta\gamma_5. \end{aligned}$$

Correspondingly, the field equations are

$$[i\gamma^\alpha D_\alpha - (M_\Delta - g_{\sigma\Delta}\sigma)]\Delta_\mu = 0, \quad (4)$$

$$D_\alpha\Delta^\alpha = 0, \quad \gamma_\alpha\Delta^\alpha = 0. \quad (5)$$

Concerning leptons, we take them as noninteracting particles and the corresponding Lagrangian density reads

$$L_l = \sum_l \bar{l}(i\gamma_\mu \partial^\mu - m_l)l. \quad (6)$$

The energy-momentum tensor is defined by

$$T_{\mu\nu} = -g_{\mu\nu}L + \sum_{B=N,\Delta} \frac{\partial B}{\partial x^\nu} \frac{\partial L}{\partial(\partial B/\partial x_\mu)}, \quad (7)$$

The propagators  $G^N(p)$  and  $G_{\alpha\beta}^\Delta(p)$  can be derived from Eqs. (2) and (3) in the mean-field approximation

$$\begin{aligned} G^N(p) &= (\not{p} + M_N^*) \left( \frac{1}{p^2 - M_N^{*2} + i\epsilon} + \frac{i\pi}{E_N^*(p)} \right) \\ &\quad \times \delta\{[p_0 - E_N^*(p)]\} f_N(p), \end{aligned} \quad (8)$$

$$\begin{aligned} G_{\alpha\beta}^\Delta(p) &= (\not{p} + M_\Delta^*) D_{\alpha\beta} \left( \frac{1}{p^2 - M_\Delta^{*2} + i\epsilon} + \frac{i\pi}{E_\Delta^*(p)} \right) \\ &\quad \times \delta\{[p_0 - E_\Delta^*(p)]\} f_\Delta(p), \end{aligned}$$

where  $f_N$  and  $f_\Delta$  are the Fermi-Dirac functions for nucleon,  $\Delta$  isobars in thermal equilibrium, respectively, and  $D_{\alpha\beta}$  can be expressed as [28]

$$D_{\alpha\beta} = g_{\alpha\beta} - \frac{1}{3}\gamma_\alpha\gamma_\beta - \frac{1}{3M_\Delta^*}(\gamma_\alpha p_\beta - \gamma_\beta p_\alpha) - \frac{2}{3M_\Delta^{*2}}p_\alpha p_\beta. \quad (9)$$

Then for a uniform system at rest, the thermodynamical potential per unit volume for hadronic matter can be evaluated from Eqs. (7) and (8), along the line proposed in Ref. [29], as

$$\begin{aligned} \frac{\Omega}{V} = -p &= -\frac{1}{3}\langle T_{ii} \rangle \\ &= \frac{1}{2}m_\sigma^2\sigma_0^2 + \frac{1}{3}bM_N(g_{\sigma N}\sigma_0)^3 + \frac{1}{4}c(g_{\sigma N}\sigma_0)^4 \\ &\quad - \frac{1}{2}m_\omega^2\omega_0^2 - \frac{1}{2}m_\rho^2\rho_0^2 + \frac{i}{3} \int \frac{d^4k}{(2\pi)^4} \\ &\quad \times \text{Tr}[k_i\gamma_i(G^N + G_\mu^{\Delta\mu})] \\ &= \frac{1}{2}m_\sigma^2\sigma_0^2 + \frac{1}{3}bM_N(g_{\sigma N}\sigma_0)^3 + \frac{1}{4}c(g_{\sigma N}\sigma_0)^4 \\ &\quad - \frac{1}{2}m_\omega^2\omega_0^2 - \frac{1}{2}m_\rho^2\rho_0^2 - T \sum_{B=N,\Delta} \gamma_B \int \frac{d^3k}{(2\pi)^3} \\ &\quad \times \ln[1 + e^{-\beta(E_B^* - \mu_B^*)}], \end{aligned} \quad (10)$$

where  $\sigma_0$ ,  $\omega_0$ , and  $\rho_0$  are the expectation values of the  $\sigma$ ,  $\omega$ , and  $\rho$  meson fields in the mean-field approximation respectively and can be easily obtained by minimizing the  $\Omega/V$ .  $\gamma_B$  is the spin degeneracy factor with  $\gamma_N = 2$  and  $\gamma_\Delta = 4$ . The inverse temperature is denoted by  $\beta = 1/T$ .  $E_B^* = (k^2 + M_B^{*2})^{1/2}$  with  $M_B^* = M_B - g_{\sigma B}\sigma_0$  denoting the effective mass of baryon  $B$ . The quantity  $\mu_i^*$  is related to the usual chemical potential  $\mu_i$  by  $\mu_i^* = \mu_i - g_{i\omega}\omega_0 - g_{i\rho}t_{3i}\rho_0$ , where  $t_{3i}$  is the third component of the isospin for the baryon  $i = N, \Delta$ . In the  $\beta$  equilibrium, the chemical potentials for the baryons satisfy

$$\mu_i = b_i\mu_n - q_i(\mu_e - \mu_\nu), \quad (11)$$

where  $b_i$  is the baryon number of particle  $i$  and  $q_i$  is its charge. We take the lepton number density fraction  $Y_{Le} = Y_e + Y_{\nu_e}$  to be 0.4 to constrain  $\mu_{\nu_e}$  in the case of that the neutrinos are trapped [30]. If the neutrinos are not trapped, we have  $\mu_{\nu_e} = 0$  in Eq. (11). There are two additional conditions that are connected with the total baryon density  $n_B$  and charge neutrality and given as

$$\begin{aligned} \sum_{i=N,\Delta} n_i &= n_B, \\ \sum_{i=N,\Delta} q_i n_i &= - \sum_{l=e^-, \mu^-} q_l n_l. \end{aligned} \quad (12)$$

Following Refs. [16,23], we have the neutrino scattering differential cross section per unit volume of matter

$$\frac{1}{V} \frac{d^3\sigma}{d^2\Omega' dE'_\nu} = - \frac{G_F}{128\pi^3} \frac{E'_\nu}{E_\nu} \text{Im}(L_{\mu\nu} \Pi^{\mu\nu}) \frac{1 - f(E_\nu)}{1 + \exp(-q_0/T)}, \quad (13)$$

where  $E_\nu, E'_\nu$  are the initial and final neutrino energies, respectively.  $G_F = 1.023 \times 10^{-5}/M_N^2$  is the weak coupling constant with  $M_N$  being the bare mass of nucleon. The function  $f(E'_\nu)$  denotes the final neutrino distribution function, which in thermal equilibrium is given as the Fermi-Dirac function

$$f(E'_\nu) = \left[ 1 + \exp\left(\frac{E'_\nu - \mu'_\nu}{T}\right) \right]^{-1}. \quad (14)$$

The neutrino tensor  $L_{\mu\nu}$  is

$$L_{\mu\nu} = 8[2k_\mu k_\nu + (k \cdot q)g_{\mu\nu} - (k_\mu q_\nu + q_\mu k_\nu) - i\epsilon_{\mu\nu\alpha\beta} k^\alpha q^\beta], \quad (15)$$

where  $k$  is the initial neutrino four-momentum and  $q = (q_0, \vec{q})$  is the four-momentum transfer. The polarization tensor  $\Pi_{\mu\nu}$  for nucleon can be found in Refs. [15,16,23]. Taking Eq. (5) into account, one can infer that most of the  $\Delta$ -neutrino couplings are canceled. The polarization tensor  $\Pi_{\mu\nu}$  for  $\Delta$  can then be written as

$$\Pi_{\mu\nu}^\Delta(q) = -i \int \frac{d^4p}{(2\pi)^4} \text{Tr}[G_{\alpha\beta}^\Delta(p) J_\mu G^{\Delta\alpha\beta}(p+q) J_\nu], \quad (16)$$

where the form of current operator of the  $\Delta$  is similar to that used for the nucleon,  $J_\mu = \gamma_\mu(C_V - C_A\gamma_5)$ , where  $C_V$  and  $C_A$  for each  $\Delta$  species are listed in Table I. One can decompose the polarization into the contributions of vector, axial, and

TABLE I. Neutral-current vector and axial coupling constants of the  $\Delta$ s with  $\sin^2\theta_W = 0.23$ . The vector coupling constants of the  $\Delta$ s are obtained from constituent quark models. The magnitudes of axial couplings of  $\Delta$ s are taken to be 1 for simplicity.

Reaction	$C_V$	$C_A$
$\nu\Delta^{++} \rightarrow \nu\Delta^{++}$	$3 - 8\sin^2\theta_W$	1
$\nu\Delta^+ \rightarrow \nu\Delta^+$	$1 - 4\sin^2\theta_W$	1
$\nu\Delta^0 \rightarrow \nu\Delta^0$	-1	-1
$\nu\Delta^- \rightarrow \nu\Delta^-$	$-3 + 4\sin^2\theta_W$	-1

vector-axial as

$$\Pi_{\mu\nu}^\Delta = C_V^2 \Pi_{\mu\nu V}^\Delta + C_A^2 \Pi_{\mu\nu A}^\Delta - 2C_V C_A \Pi_{\mu\nu VA}^\Delta. \quad (17)$$

According to the principles of vector current conservation and translational invariance, one can expand the  $\Pi_{\mu\nu V}^\Delta$  in terms of two independent components, referred to as  $\Pi_L^\Delta$  and  $\Pi_T^\Delta$ .  $\Pi_{\mu\nu A}^\Delta$  and  $\Pi_{\mu\nu VA}^\Delta$  can be expressed as

$$\Pi_{\mu\nu A}^\Delta = \Pi_{\mu\nu V}^{\Delta'} + g_{\mu\nu} \Pi_A^\Delta, \quad (18)$$

$$\Pi_{\mu\nu VA}^\Delta = i\epsilon_{\mu,\nu,\alpha,0} q^\alpha \Pi_{VA}^\Delta,$$

where the related  $\Pi_{\mu\nu V}^{\Delta'}$  can also be written in terms of two independent components, referred to as  $\Pi_L^{\Delta'}$  and  $\Pi_T^{\Delta'}$ . The derivations and the expressions of these two polarization factors are lengthy and some of them are listed in the Appendix.

The total cross section per unit volume can be obtained by integrating Eq. (13) over the final neutrino energies and scattering angles with a transformation  $2\pi q dq dq_0 = E_\nu E'_\nu d^2\Omega' dE'_\nu$  and given as

$$\frac{\sigma}{V} = 2\pi \int_{-\infty}^{E_\nu} dq_0 \int_{|q_0|}^{2E_\nu - q_0} dq \frac{q}{E_\nu E'_\nu} \frac{1}{V} \frac{d^3\sigma}{d^2\Omega' dE'_\nu}. \quad (19)$$

### III. RESULTS AND DISCUSSION

In this work, we take a set of parameters from the so-called GM3 model [4], listed in Table II, from which the properties of nuclear matter in equilibrium are given as follows: the incompressibility, the symmetry energy, the saturation density, the binding energy per nucleon in the matter, and the ratio of the effective mass of nucleon to the bare one are 240 MeV, 32.5 MeV,  $0.153 \text{ fm}^{-3}$ ,  $-16.3 \text{ MeV}$ , and 0.78, respectively. The  $\Delta$ - $\sigma$  coupling is related to the N- $\sigma$  one by  $g_{\sigma\Delta} = 1.3g_{\sigma N}$  according to the result of QCD sum rules [10] or from the assumption that  $g_{\sigma\Delta}/g_{\sigma N} \sim M_\Delta/M_N$  [1]. Moreover,  $g_{\omega\Delta}$  and  $g_{\rho\Delta}$  are taken to be identical with  $g_{\omega N}, g_{\rho N}$ , respectively.

In Fig. 1, we illustrate the calculated results of the particle populations as a function of density in neutrino-free matter at  $\beta$  equilibrium and zero temperature. The upper panel shows the result of the matter in which the baryons are only nucleons. The lower panel corresponds to the case that the  $\Delta$  degrees of freedom are included. The upper panel of Fig. 1 shows that the fractions of proton and leptons grow smoothly with the increase of the matter. It implies that the electron chemical potential increases monotonically as a function of the density. However, when the  $\Delta$ s are taken into account, the result shown in the lower panel of Fig. 1 presents evidently a threshold behavior, i.e.,  $\Delta^-$ s emerge suddenly at the density  $\rho \simeq 0.3 \text{ fm}^{-3}$ . Because of the negativity of their charge, they replace the electrons to a certain extent to achieve the charge neutrality. As a consequence, the electron fraction decreases a little with

TABLE II. Nucleon-meson coupling constants in the GM3 model.

$g_\sigma/m_\sigma$ (fm)	$g_\omega/m_\omega$ (fm)	$g_\rho/m_\rho$ (fm)	$b$	$c$
3.1507	2.1954	2.1888	0.008659	-0.002421

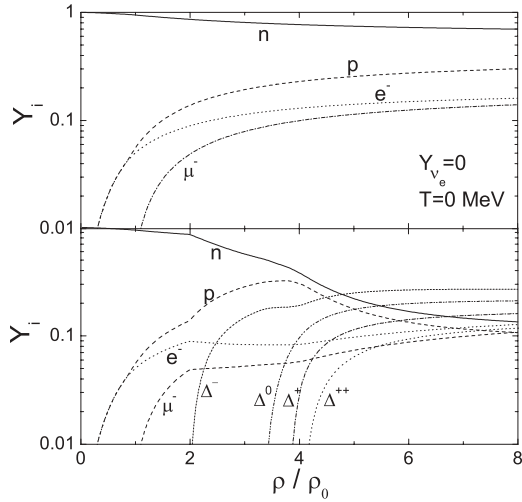


FIG. 1. Calculated results of the fractions of the ingredients of neutron star matter at  $T = 0$  MeV in the GM3 model of parameters (The upper, lower panel corresponds to the matter without, with the  $\Delta$  degrees of freedom, respectively).

the increase of the density until the  $\Delta^{++}$ s appear where the electron fraction turns to increase again. Moreover the fraction of proton reaches its maximum at  $\rho \simeq 0.62 \text{ fm}^{-3}$ . Comparing the presently obtained results with those of the calculations for neutron star matter, including hyperons (see, for example, Ref. [31]), an obvious distinction is that the fraction of  $\mu^-$  does not decrease with the increase of the density even after  $\Delta^-$ s appear. It indicates that the electron chemical potential grows monotonically. This may mainly result from the high isospin of the  $\Delta^-$  that could have significant effects on the condensate of the negatively charged mesons in neutron stars [30]. In addition, it is also worth mentioning that the presently obtained sequence of the appearance of the  $\Delta$  species is consistent with the notion of charge-favored or unfavored species [8], that is, the first  $\Delta$  species to appear is the  $\Delta^-$ , followed by the  $\Delta^0$  and the  $\Delta^+$ , then the  $\Delta^{++}$ .

To show the effects of neutrino trapping on the property of neutron star matter, we have evaluated the fractions of various species in the neutron star matter at temperature  $T = 30$  MeV in the cases without and with neutrinos being trapped. The obtained results are illustrated in the left and right panels of Fig. 2, respectively. Furthermore, the upper panels present the results for the matter in which the baryons are only nucleons, and the lower panels correspond to those in the matter with  $\Delta$ s. Comparing Fig. 2 with Fig. 1, one can recognize easily that the finite temperature smooths the threshold behavior and favors the presence of  $\Delta$ s (lower left panel). The increase of the density weakens the effects of temperature. Moreover, in the case of with neutrinos being trapped (as shown in the lower right panel), the neutrino trapping delays the appearance of the negatively charged  $\Delta$  species (i.e., it emerges at higher density). In addition, the fraction of the neutrino  $\nu_e$  decreases smoothly with the increase of density at finite temperature, which is different from the behavior in the matter including hyperons [30].

From the above discussion, one can notice that the  $\Delta$  species appear at moderate density in the case of presently

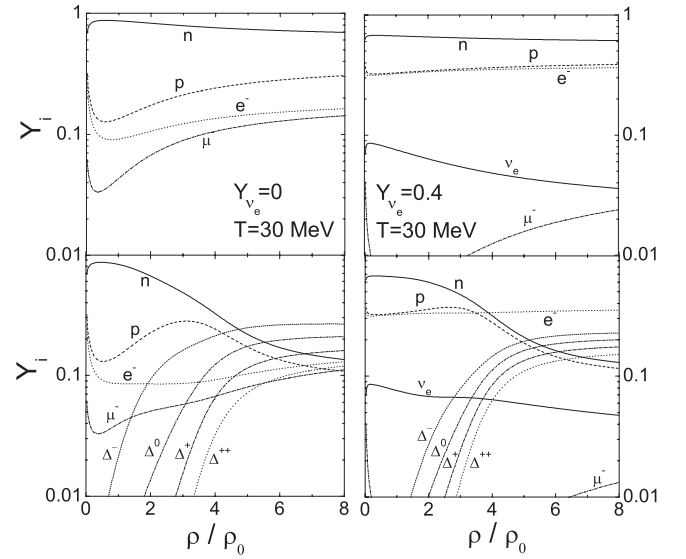


FIG. 2. Calculated fractions of the composition of neutron star matter without (upper panels) and with (lower panels) the  $\Delta$  degrees of freedom at  $T = 30$  MeV in the GM3 model of parameters; (left) results for neutrino-free matter; (right) results for neutrino-trapped matter.

used parameters and become more important components of neutron star matter at high density. Hence they may contribute to the neutrino scattering rates. We calculate then the differential cross sections per unit volume of the scatterings between neutrino and the baryons and other leptons and the mean-free paths of neutrinos in the matter as well in the cases mentioned above. The obtained results of the neutrino scattering differential cross sections with each ingredient in the matter at  $\rho = 4\rho_0 = 0.612 \text{ fm}^{-3}$  and zero temperature for a neutrino with energy  $E_\nu = 5$  MeV and fixed momentum transfer  $|\mathbf{q}| = 2.5$  MeV, as a function of  $q_0/|\mathbf{q}|$ , are shown in Fig. 3. Because the calculations indicate that the influence of the  $\mu^-$  is negligibly small, we do not illustrate the corresponding results in Fig. 3 and the following. Considering the matter with the baryons being only nucleons, one can see from the left panel of Fig. 3 that the scattering between neutrino and neutron is the dominate process in the low  $q_0$  region and that between neutrino and electron becomes the dominate one in high  $q_0$  region. In the matter that includes  $\Delta$ s, the results shown in the right panel of Fig. 3 manifest that the contribution of the scattering between neutrino and  $\Delta^{++}$  to the cross section is absent and those from  $\Delta^-$ ,  $\Delta^0$ , and  $\Delta^+$  are all in the low  $q_0$  region. Such a phenomenon arises from the kinetic restriction and Pauli blocking. In more detail, comparing the right panel with the left panel, one can recognize evidently that the  $\Delta^-$  replaces the neutron to dominate the contributions to the cross section. Such a result is quite similar to that of the  $\Sigma^-$  in the matter with hyperons [15]. Along the line proposed in Ref. [15], one can understand such a feature as mainly the consequence of the greater effective chemical potential of the  $\Delta^-$  for its negative charge and larger vector coupling constant with neutrinos. To understand such results more thoroughly, we look through the longitudinal and the transverse polarizations  $-\text{Im}\Pi_L$  and  $-\text{Im}\Pi_T$  of the ingredients  $n$ ,  $p$ ,

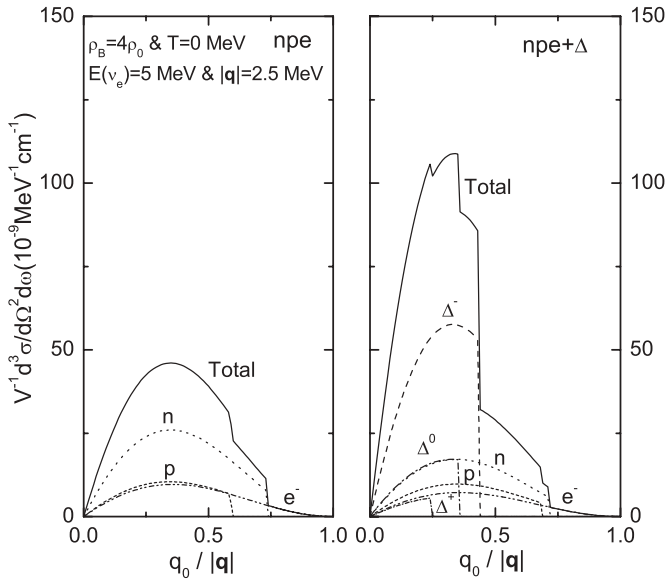


FIG. 3. Calculated differential cross sections of the scatterings between neutrino and the ingredients of neutron star matter without (left panel) and with (right panel) the  $\Delta$  degrees of freedom at  $T = 0$  MeV.

$e^-$ , and  $\Delta$ s in the matter. The calculated results are displayed in Fig. 4. In this figure the curves labeled  $\Delta$  with no superscript represent the polarizations of a fictitious particle with the spin of  $\Delta$  but with the mass and effective chemical potential of neutron. The figure manifests apparently that the polarization magnitudes of such a hypothetical particle are almost two times of those of neutron. Comparing the characteristic of this fictitious particle and that of neutron, we can infer that

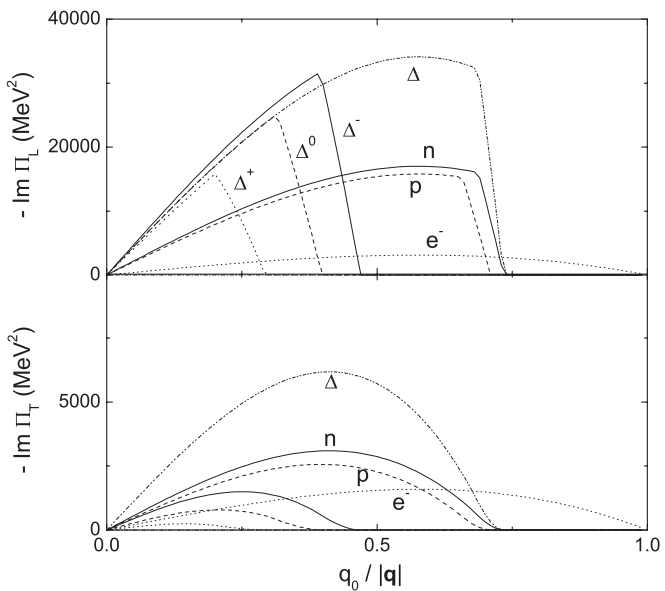


FIG. 4. Calculated imaginary parts of the longitudinal and transverse polarizations for  $n$ ,  $p$ ,  $e^-$ , and  $\Delta$ s at temperature  $T = 0$ . The curves labeled  $\Delta$  without any superscript represent the results of a fictitious particle with the spin of  $\Delta$  but the mass and effective chemical potential of neutron.

the great enhancement of the polarization comes from the high spin ( $s_\Delta = 3/2$ ,  $s_N = 1/2$ ). These indicate that the much larger scattering cross section on the  $\Delta^-$  results from both the phase space (or the degeneracy of the spin space) and the effective chemical potential and the vector coupling constant with neutrinos. Note that the  $\Delta$  polarizations are also sensitive to the  $\Delta$  effective masses and effective chemical potentials. One can expect that, when we impose the practical values of the effective masses and effective chemical potentials on the  $\Delta$ s, the polarizations will shrink to lower energy transfer  $q_0$ . The variation characteristic of the curves displayed in Fig. 4 confirms such an understanding evidently. The obvious suppression of the transverse responses (shown in the lower panel of Fig. 4) provides also an understanding of the weak response of the  $\Delta^+$  and the approximately same magnitude of the  $\Delta^0$  as that of the neutron in the low  $q_0$  region.

To investigate the medium effects of matter more thoroughly, we have also calculated the differential cross sections of the neutrino scattering on the particles in the neutron star matter at temperature  $T = 30$  MeV. The obtained results are illustrated in Fig. 5, in which the upper and lower panels show the results of “free” neutrinos (here the “free” means that with zero chemical potential but the matter is still in thermal equilibrium) and those of trapped neutrinos, respectively, the left and right panels display the results in the matter with the baryons being only nucleons and with both nucleons and  $\Delta$ s, respectively. From the upper panels, one can notice that finite temperature opens the  $q_0 < 0$  responses and increases the neutrino reaction energy to about  $\pi T$ , enhancing considerably the neutrino scattering cross section in comparison with those at zero temperature. In the case of that neutrinos are trapped and degenerate, the energies of the scattering neutrinos are mainly concentrated in the region close to their chemical potential ( $\mu_{\nu_e} \sim 250$  MeV, corresponding to the typical density of neutron star matter), and the differential cross sections are enlarged compared to those in the neutrino-free case in which the neutrino reaction energy is about 100 MeV (smaller than the  $\mu_{\nu_e}$ ). Furthermore, as the  $\Delta$  degrees of freedom are taken into account, the  $\Delta$  isobars enhance the scattering cross sections obviously, where the contribution from  $\Delta^-$  is dominant, and from  $\Delta^0$  is comparable to that comes from nucleon.

Another quantity characterizing the neutrino transportation is its mean free path  $\lambda$ , which is simply related to Eq. (19) by  $\lambda = (\sigma/V)^{-1}$ . One can expect that, as the  $\Delta$  degrees of freedom are included, the mean free path will decrease and the opacity of the neutron star matter will increase, because the  $\Delta$ s open additional channels for neutrino scattering to take place. The calculated results of the mean free path of the neutrinos in the matter at temperature  $T = 0$  with neutrino energy  $E = 5$  MeV and that at  $T = 30$  MeV with  $E = 100$  MeV are represented in the top, middle panels of Fig. 6 respectively, and those of the trapped neutrinos in the matter at  $T = 30$  MeV and with  $E = \mu_{\nu_e}$  are shown in the bottom panel. From Fig. 6, one sees apparently that the mean-free paths of the neutrinos at finite temperatures is substantially reduced compared to the corresponding values at zero temperature. And that in the neutrino-trapped case decreases more rapidly with increasing density in the presence of the  $\Delta$ s (lower panel) than those in the other two cases.

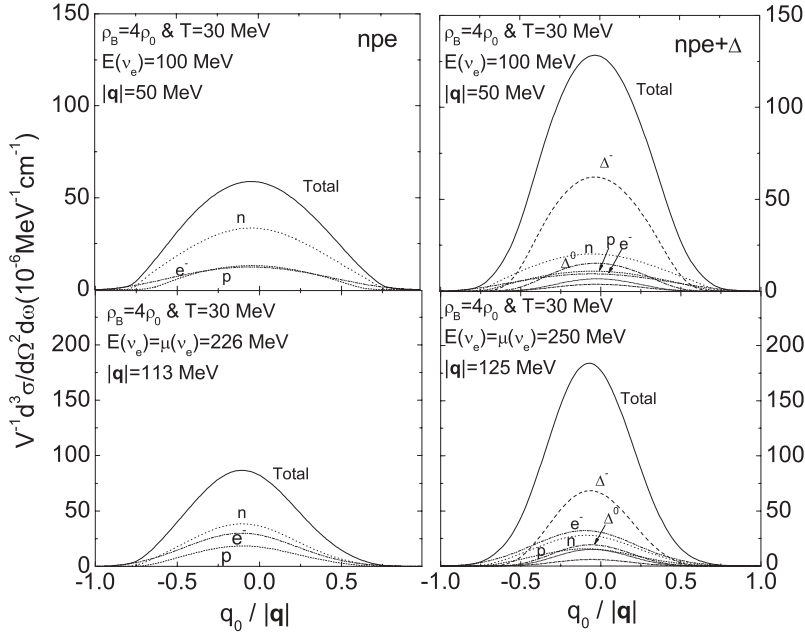


FIG. 5. Calculated differential cross sections of the scatterings between neutrino and the ingredients of neutron star matter without (left panels) and with (right panels) the  $\Delta$  degrees of freedom at  $T = 30$  MeV; (upper panels) results for neutrino-free matter; (lower panels) results for neutrino-trapped matter.

#### IV. SUMMARY

In summary, we have investigated the components of neutron star matter and the scattering cross sections of neutrinos on the ingredients of the matter in an effective hadronic theory in this article. Although there exists uncertainty in the  $\Delta$ -meson coupling constants, our calculation indicates that the  $\Delta$  isobars may emerge in neutron star matter if the coupling constants are taken to be those predicted in the finite-density QCD sum rules. The appearance of the  $\Delta$ s does not cause a decline of the electron chemical potential as the matter density increases, even in the presence of negatively charged particle (i.e., the  $\Delta^-$ ). Neutrinos, when trapped, delay the appearance of the  $\Delta$ s. The large vector coupling between  $\Delta^-$  and neutrino and the higher

spin of  $\Delta$ s affect greatly the neutrino scattering cross section and induce the contribution of  $\Delta^-$  to be dominate at high density. The calculations also manifest that finite temperature influences the components of neutron star matter slightly but enhances the neutrino scattering cross sections significantly. Moreover, neutrino trapping leads to drastic decline of the mean free path of neutrinos in the neutron star matter including  $\Delta$  isobars.

Because hyperons have the similar masses of the  $\Delta$ s, they should be included in the investigation of the properties of neutron stars for completeness. Moreover, we have taken only the neutral-current reaction effect of the  $\Delta$ s into account when calculating the neutrino scattering cross sections in this work. In fact, the charged-current reactions may contribute to the neutrino scattering and the opacity of the matter as well. The studies on these aspects are necessary and in progress.

#### ACKNOWLEDGMENTS

This work was supported by the National Natural Science Foundation of China under contract Nos. 10425521, 10435080, 10575004 and 10575005, the Key Grant Project of Chinese Ministry of Education (CMOE) under contract No. 305001, and the Research Fund for the Doctoral Program of Higher Education of China under grant No. 20040001010. One of the authors (Y.X.L.) thanks also the support of the Foundation for University Key Teacher by the CMOE.

#### APPENDIX

In this appendix we present the imaginary parts of the polarizations of the  $\Delta$  isobars used in this article

$$\text{Im}\Pi_L^\Delta(q_0, \mathbf{q}) = \frac{\lambda_\Delta}{36\pi} \frac{q_\mu^2}{|\mathbf{q}|^3} \int_{\varepsilon_-}^{\infty} dE \left[ \left( 9 - \frac{2q_\mu^2}{M_\Delta^{*2}} + \frac{q_\mu^4}{2M_\Delta^{*4}} \right) \times \left( E + \frac{q_0}{2} \right)^2 - \left( 5 - \frac{2q_\mu^2}{M_\Delta^{*2}} + \frac{q_\mu^4}{2M_\Delta^{*4}} \right) \frac{|\mathbf{q}|^2}{4} \right]$$

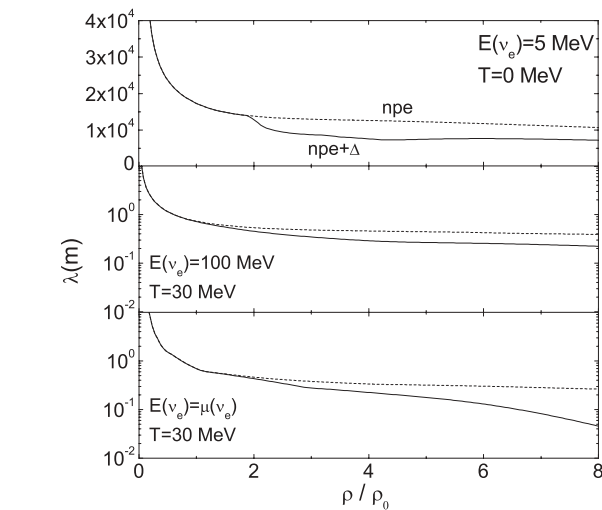


FIG. 6. Calculated mean free path of neutrinos in neutron star matter with and without the  $\Delta$  degrees of freedom at  $T = 0$  MeV (upper panel) and  $T = 30$  MeV (middle and lower panels). The upper and middle panels refer to the cases in which neutrinos are free. The lower panel corresponds to that the neutrinos are trapped.

$$\begin{aligned}
& \times [F^+(E, E + q_0) + F^+(E + q_0, E)], \\
\text{Im}\Pi_T^\Delta(q_0, \mathbf{q}) &= \frac{\lambda_\Delta}{72\pi} \frac{q_\mu^2}{|\mathbf{q}|^3} \int_{\varepsilon_-}^{\infty} dE \left\{ \left( 9 - \frac{2q_\mu^2}{M_\Delta^{*2}} + \frac{q_\mu^4}{2M_\Delta^{*4}} \right) \right. \\
& \times \left[ \left( E + \frac{q_0}{2} \right)^2 + \frac{|\mathbf{q}|^2 M_\Delta^{*2}}{q_\mu^2} \right] \\
& \left. + \left( 1 - \frac{2q_\mu^2}{M_\Delta^{*2}} + \frac{q_\mu^4}{2M_\Delta^{*4}} \right) \frac{|\mathbf{q}|^2}{4} \right\} \\
& \times [F^+(E, E + q_0) + F^+(E + q_0, E)], \\
\text{Im}\Pi_L^{\Delta'}(q_0, \mathbf{q}) &= \frac{\lambda_\Delta}{36\pi} \frac{q_\mu^2}{|\mathbf{q}|^3} \int_{\varepsilon_-}^{\infty} dE \left[ \left( 5 - \frac{2q_\mu^2}{M_\Delta^{*2}} + \frac{q_\mu^4}{2M_\Delta^{*4}} \right) \right. \\
& \times \left( E + \frac{q_0}{2} \right)^2 - \left( 4 - \frac{2q_\mu^2}{M_\Delta^{*2}} + \frac{q_\mu^4}{2M_\Delta^{*4}} \right) \frac{|\mathbf{q}|^2}{4} \left. \right] \\
& \times [F^+(E, E + q_0) + F^+(E + q_0, E)], \\
\text{Im}\Pi_T^{\Delta'}(q_0, \mathbf{q}) &= \frac{\lambda_\Delta}{72\pi} \frac{q_\mu^2}{|\mathbf{q}|^3} \int_{\varepsilon_-}^{\infty} dE \left\{ \left( 5 - \frac{2q_\mu^2}{M_\Delta^{*2}} + \frac{q_\mu^4}{2M_\Delta^{*4}} \right) \right. \\
& \times \left[ \left( E + \frac{q_0}{2} \right)^2 + \frac{|\mathbf{q}|^2 M_\Delta^{*2}}{q_\mu^2} \right] \\
& \left. + \left( 3 - \frac{2q_\mu^2}{M_\Delta^{*2}} + \frac{q_\mu^4}{2M_\Delta^{*4}} \right) \frac{|\mathbf{q}|^2}{4} \right\} \\
& \times [F^+(E, E + q_0) + F^+(E + q_0, E)], \\
\text{Im}\Pi_A^\Delta(q_0, \mathbf{q}) &= \frac{\lambda_\Delta}{72\pi} \frac{M_\Delta^{*2}}{|\mathbf{q}|} \int_{\varepsilon_-}^{\infty} dE \left( 9 - \frac{4q_\mu^2}{M_\Delta^{*2}} + \frac{q_\mu^4}{M_\Delta^{*4}} \right) \\
& \times [F^+(E, E + q_0) + F^+(E + q_0, E)], \\
\text{Im}\Pi_{VA}^\Delta(q_0, \mathbf{q}) &= \frac{\lambda_\Delta}{72\pi} \frac{q_\mu^2}{|\mathbf{q}|^3} \int_{\varepsilon_-}^{\infty} dE \left( E + \frac{q_0}{2} \right) \\
& \times \left( 5 - \frac{2q_\mu^2}{M_\Delta^{*2}} + \frac{q_\mu^4}{2M_\Delta^{*4}} \right) [F^-(E, E + q_0) \\
& \left. + F^-(E + q_0, E)], \tag{A1}
\end{aligned}$$

where the spin degeneracy factor  $\lambda_\Delta = 4$ . The lower cutoff  $\varepsilon_-$  and the function  $F^\pm(E_1, E_2)$  appeared above are the same as those given in Ref. [15].

- 
- [1] B. M. Waldhauser, J. Theis, J. A. Maruhn, H. Stöcker, and W. Greiner, Phys. Rev. C **36**, 1019 (1987).  
[2] Z. X. Li, G. J. Mao, Y. Z. Zhuo, and W. Greiner, Phys. Rev. C **56**, 1570 (1997).  
[3] X. Hu and H. Guo, Phys. Rev. C **67**, 038801 (2003).  
[4] N. K. Glendenning and S. A. Moszkowski, Phys. Rev. Lett. **67**, 2414 (1991).  
[5] N. K. Glendenning, *Compact Stars* (Springer-Verlag, New York, 2000).  
[6] J. M. Lattimer and M. Prakash, Astrophys. J. **550**, 426 (2001).  
[7] F. Weber, Prog. Part. Nucl. Phys. **54**, 193 (2005).  
[8] N. K. Glendenning, Astrophys. J. **293**, 470 (1985).  
[9] N. K. Glendenning, F. Weber, and S. A. Moszkowski, Phys. Rev. C **45**, 844 (1992).  
[10] X. Jin, Phys. Rev. C **51**, 2260 (1995).  
[11] D. S. Kosov, C. Fuchs, B. V. Martemyanov, and A. Faessler, Phys. Lett. **B421**, 37 (1998).  
[12] F. Weber and M. K. Weigel, Nucl. Phys. **A505**, 779 (1989).  
[13] H. Huber, F. Weber, M. K. Weigel, and Ch. Schaab, Int. J. Mod. Phys. E **7**, 301 (1998).  
[14] C. J. Horowitz and M. A. Pérez-García, Phys. Rev. C **68**, 025803 (2003).  
[15] S. Reddy and M. Prakash, Astrophys. J. **478**, 689 (1997).  
[16] S. Reddy, M. Prakash, and J. M. Lattimer, Phys. Rev. D **58**, 013009 (1998).  
[17] S. Reddy, M. Prakash, J. M. Lattimer, and J. A. Pons, Phys. Rev. C **59**, 2888 (1999).  
[18] R. F. Sawyer, Phys. Rev. D **11**, 2740 (1975).  
[19] R. F. Sawyer, Phys. Rev. C **40**, 865 (1989).  
[20] N. Iwamoto and C. J. Pethick, Phys. Rev. D **25**, 313 (1982).  
[21] C. J. Horowitz and K. Wehrberger, Nucl. Phys. **A531**, 665 (1991).  
[22] C. J. Horowitz and K. Wehrberger, Phys. Rev. Lett. **66**, 272 (1991).  
[23] C. J. Horowitz and K. Wehrberger, Phys. Lett. **B266**, 236 (1991).  
[24] J. A. Pons, S. Reddy, M. Prakash, J. M. Lattimer, and J. A. Miralles, Astrophys. J. **513**, 780 (1999).  
[25] B. D. Serot and J. D. Walecka, The Relativistic Nuclear Many-body Problem, in *Advances in Nuclear Physics*, edited by J. W. Negele and E. Vogt (Plenum Press, New York, 1986), Vol. 16, p. 1.  
[26] K. Johnson and E. C. G. Sudarshan, Ann. Phys. **13**, 126 (1961).  
[27] W. Rarita and J. Schwinger, Phys. Rev. **60**, 61 (1941).  
[28] F. de Jong and R. Malfiet, Phys. Rev. C **46**, 2567 (1992).  
[29] R. J. Furnstahl and B. D. Serot, Phys. Rev. C **41**, 262 (1990).  
[30] M. Prakash, I. Bombaci, P. J. Ellis, J. M. Lattimer, and R. Knorren, Phys. Rep. **280**, 1 (1997).  
[31] M. Hanauske, D. Zschesche, S. Pal, S. Schramm, H. Stöcker, and W. Greiner, Astrophys. J. **537**, 958 (2000).